Foam flow in a model porous medium
II. the effect of trapped gas

Jones, S. A.; Getrouw, N.; Vincent-Bonnieu, S.

DOI
10.1039/c7sm02458d

Publication date
2018

Document Version
Accepted author manuscript

Published in
Soft Matter

Journal Name

ARTICLE

Foam Flow in a Model Porous Medium : II. The Effect of Trapped Gas

Received 00th January 20xx,
Accepted 00th January 20xx

DOI: 10.1039/x0xx00000x

www.rsc.org/

S.A. Jones,[a,†] N. Getrouw[a] and S. Vincent-Bonnieu[a,b]

Gas trapping is an important mechanism in both Water or Surfactant Alternating Gas (WAG/SAG) and foam injection processes in porous media. Foams for enhanced oil recovery (EOR) can increase sweep efficiency as they decrease the gas relative permeability, and this is mainly due to gas trapping. However, gas trapping mechanisms are poorly understood. Some studies have been performed during corefloods, but little work has been carried out to describe the bubble trapping behaviour at the pore scale. We have carried out foam flow tests in a micromodel etched with an irregular hexagonal pattern. Image analysis of the foam flow allowed the bubble centres to be tracked and local velocities to be obtained. It was found that the flow in the micromodel is dominated by intermittency and localized zones of trapped gas. The quantity of trapped gas was measured both by considering the fraction of bubbles that were trapped (via velocity thresholding) and by measuring the area fraction containing immobile gas (via image analysis). A decrease in the quantity of trapped gas was observed for both increasing total velocity and increasing foam quality. Calculations of the gas relative permeability were made with the Brooks Corey equation, using the measured trapped gas saturations. The results showed a decrease in gas relative permeabilities, and gas mobility, for increasing fractions of trapped gas. It is suggested that the shear thinning behaviour of foam could be coupled to the saturation of trapped gas.

Introduction

We have previously discussed foam coarsening in porous media[1], a process which leaves the majority of the foam lamellae residing in minimum energy configurations in the pore throats. Once lamellae are in these low energy configurations, there is a greater resistance to restarting flow, and the bubble formed by these lamellae effectively traps gas in the pore. Gas trapping is an important gas mechanism that occurs during Water/Surfactant Alternating Gas (WAG/SAG) and foam injection processes. When gas is trapped in place, the overall gas mobility is reduced, which then reduces the relative permeability of the gas phase[2,3,4].

Although trapped gas is of great importance in the understanding of foam behaviour in a porous media, there are only a few experimental studies on this subject, probably due to the technical challenges involved in differentiating between stationary and moving gas within a rock core. Most studies have focused on injecting a foam, then once steady state flow has been obtained a tracer gas is injected with the foam. The quantity of trapped gas can then be determined either by using CT imaging to visualize the tracer[5,6] or by sampling the effluent to determine the concentration of tracer[7,8,9]. However, there are potential errors linked to these tracer measurement techniques due to the fact that the flow paths within the rock core can fluctuate with time. Any fluctuations can cause a false reading of the number of flowing paths that appear to be open and could thus cause an overestimation of the fraction of moving gas and an underestimation of the trapped gas fraction[6].

Even ignoring any potential underestimation, the quantity of gas trapped in a porous medium is still significant. Radke and Gillis[8] found trapped gas fractions of between 70% and 100% for all their tests, with superficial velocities in the range of 0.5 to 4 m/day and foam qualities between 0.8 and 1.0 respectively. Friedman et al.[7] also measured trapped gas fractions in the range 75% to 90% over a wide range of velocities (from 25 up to 150 m/day). In both these cases, the authors found only a small variation in the trapped gas with changing velocity, with Radke and Gillis[8] observing a slight trend towards higher values of trapped gas with higher velocities.

In contrast, Tang and Kovscek[9] found a significant decrease in trapped gas with increasing gas velocity (and a constant liquid velocity of 0.19 m/day), with the trapped gas fraction dropped from 87% at a gas velocity, u_g, of 0.55 m/day to 56% at 30.4 m/day. They also showed a dependence of the trapped gas on foam quality, with drier foams giving lower values of trapped gas.

[a] TU Delft.
[b] Shell Global Solutions International B.V.
† Corresponding author.

In order to investigate some of these issues further, we have carried out foam flow tests, with a focus on trapped gas, in a model porous medium etched on a 2D glass microfluidic chip. The advantage of working with a 2D geometry is that the foam behaviour can be easily visualised and quantified, and the number of trapped bubbles can be determined at any single time. With this experimental setup, it was possible to determine the dependency of the fraction of trapped gas on foam quality, linear velocity and location within the micromodel. In addition, the effect of the trapped gas saturation on the gas relative permeability was studied theoretically.

Experimental Method

Foam Flow Tests

Foam flow tests were carried out in a borosilicate-glass micromodel. The micromodel was etched with an irregular hexagonal pattern that formed a model porous medium, with a Gaussian distribution of pore diameters (mean = 60 µm) and throat widths (mean = 13 µm) (Figure 1). The pattern had a total width of 800 µm (10/11 pores) and an overall length of 60 mm (849 pores), with a channel depth of 5 µm. The permeability of the micromodel was determined experimentally and found to be 0.72 Darcy.

The chip was viewed using an inverted microscope (Leica DMi8) in Transmitted Light mode, with a X10 objective that allowed for the whole width of the porous channel to be observed. Images of the chip, and the foam flow through the pores, were recorded using a high speed video camera (Photron) connected to the microscope. The video images had a resolution of 1280 x 720 pixels and a typical acquisition rate of 125 frames per second was used.

The foam was generated by coinjecting surfactant solution and nitrogen gas into the micromodel through a frit with 10 µm pores. The surfactant used was a Sodium C14-16 Olefin Sulfonate (AOS) (Bioterge AS-40K) and the solution contained 0.5 wt% total active surfactant with 3 wt% NaCl in demineralized water. The surfactant solution was injected using a syringe pump fitted with a 20 ml stainless steel syringe, which gave a minimum achievable flow rate of 0.25 µL/min (equivalent to a superficial velocity of 1.04×10^{-3} m.s^{-1}). The gas injection was controlled using a mass flow controller with full scale of 0.7 ml/min. The pressure in the system was monitored using two absolute pressure transducers (60 bar full-scale, ±0.04% FS). Once a steady state foam flow was achieved in the chip, the flow behaviour was recorded using the high speed video camera.

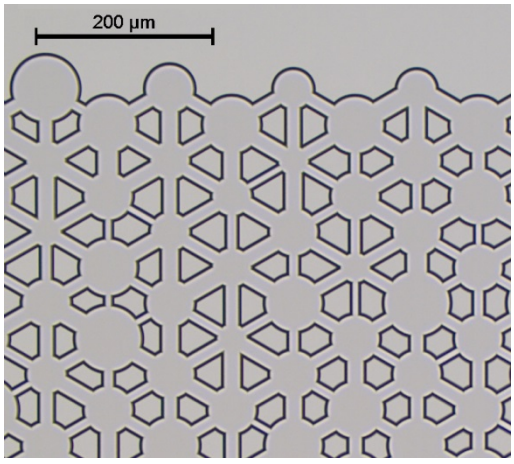

Figure 1 *Photograph of a section of the micromodel, showing the distribution of pore diameters and pore throat widths.*

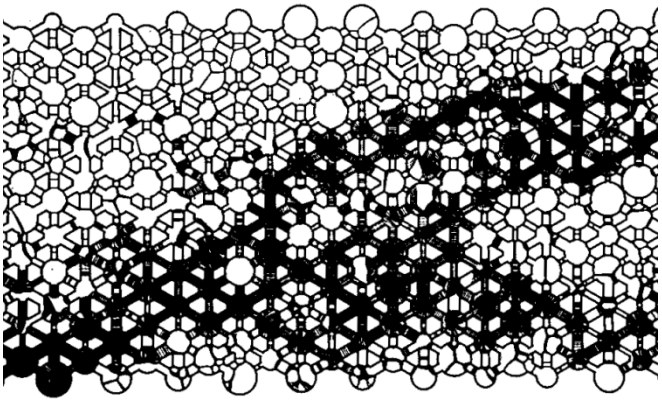

Figure 2 Composite image of 40 consecutive, binarised video frames (recorded at 125 frames per second). Regions of flow, where the lamellae have moved, show as black, and regions of trapped gas remain white.

The video images were processed and binarised using the ImageJ software package[10]. The trapped gas in the system could then be measured using two different techniques. Firstly, a composite image of multiple consecutive video frames could be generated in ImageJ (Figure 2). The regions of flow could then be identified, where the sequential images of the moving lamellae overlaid to fill the pores with black (see the solid black pore/throat domains in Figure 2). The regions of trapped gas, where the lamellae are stationary, remained white, and a simple image analysis then allowed for the quantification of the trapped gas i.e. the white areas. We could then define a ***trapped area fraction***. This trapped area is calculated as a fraction of the total pore area, so makes a direct measurement of the trapped gas saturation, S_{gt}, within the micromodel [-]. The trapped gas saturation is defined as:

$$S_{gt} = f_{gt}.S_g \quad (1)$$

where f_{gt} is the trapped gas fraction [-] and S_g is the total gas saturation [-].

Secondly, the individual bubbles were tracked and their velocities calculated. Bubbles with a velocity beneath a specific threshold were considered trapped. The threshold was determined manually for each test, dependent on the individual test conditions, and was set at a finite value (rather than 0) to avoid counting any bubbles that may have been oscillating in position while still remaining trapped in a pore, and also to filter out any small artificial velocities that may have been created during the image processing. The number of trapped bubbles was then described as a fraction of the total number of bubbles, giving a ***trapped bubble fraction***.

This gives us a direct measurement of the trapped gas fraction, f_{gt}, within the micromodel.

Using these two measurement techniques, the amount of gas trapped within the micromodel could then be measured as a function of position, flow velocity and foam quality.

Trapped Gas Model

The theory of foam flooding predicts that the gas relative permeability decreases as certain pores are blocked by trapped gas[3]. The relative permeability can capture the effect of the trapped gas via equation 2 below[2]:

$$k_{rg}^{foam} = \frac{k_{rg}(S_g,S_{gt})}{(u_l+u_g)} \quad (2)$$

where u_l and u_g are the Darcy velocities of the liquid and gas phases respectively [m.s^{-1}] and $k_{rg}(S_g)$ is the relative gas permeability. $k_{rg}(S_g,S_{gt})$ is a function of the gas saturation S_g, and has a value derived from the Brooks Corey permeability model for two phases, i.e.

$$k_{rg}(S_g,S_{gt}) = k_{rg}^0\left(\frac{S_g-S_{gt}}{1-S_{wc}-S_{gt}}\right)^{n_g}, \quad (3)$$

where the $k_{rg}{}^0$ is the endpoint relative permeability of gas [m^2], S_{wc} is the connate water saturation, S_{gt} is the connate or trapped gas saturation and n_g is the gas correlation exponent for the Brooks Corey equation.

We assumed that k_{rg} is a function of S_{gt} because, in our experiments, we observed that S_{gt} varied with flow rate and foam quality. The gas saturation, S_g, was measured directly by image processing in the microfluidic experiments. The connate, or residual, water saturation, S_{wc}, was measured in a drainage experiment during which the microchip was first saturated with water, then flooded with gas, and was found to have a value S_{wc} = 0.05 [-]. The saturation of trapped gas S_{gt} can be derived from the fraction of trapped gas f_{gt} measured in the experiment (eqn. 1). The fraction f_{gt} is measured for different Darcy velocities $u_t = u_l + u_g$ and fractional flows.

The micromodel has a permeability of 719 mD, a value similar to that of the Bentheimer sandstone (773mD) previously tested by Kapetas et al.[11]. The Corey parameters for the Bentheimer sandstone were found to be n_g = 0.7 and n_w = 2.86, and these values were used in the current model. The end point of the gas permeability is 0.59 for the Bentheimer sandstone[11]. The gas relative permeability k_{rg} can then be calculated from equations 1 and 2, using a visual, experimental measurement of the trapped fraction.

The gas relative permeability can also be derived from the experimental pressure measurements across the micromodel using equations 4 and 5.

$$\mu_{foam} = \frac{k|\nabla P|}{u_g+u_l} \quad (4)$$

where μ_{foam} is the apparent viscosity of the foam [Pa.s], k is the permeability of the porous media [m^2] and ∇P is the pressure gradient [Pa.m^{-1}]. The gas relative permeability k_{rg} can then be calculated using the Darcy law, the definition of the gas fractional flow $f_g=u_g/(u_g+u_l)$, and the gas viscosity μ_g [Pa.s], as expressed in equation 5:

$$k_{rg}(\mu_{foam}) = \frac{f_g\mu_g}{\mu_{foam}} \quad (5)$$

The gas relative permeability is calculated from the experimental measurement of the trapped gas (equations 3) and from the pressure drop (equation 5). If the Brooks Corey model is correct for the 2D micromodel, then equations 3 and 5 should give the same results.

Results and Discussion - Experiments

Initial Flow Behaviour

The initial foam flow through the micromodel showed piston-like flow behaviour, with a sharp flow front (Figure 3). The individual bubbles moved in a stop-start fashion, but this intermittency did not result in any fingering in the flow profile. As the foam front advanced further, some of the bubbles remained trapped in the pores, giving an immediate value of trapped gas within the micromodel. This value was very low however (< 5%) - in the case shown in Figure 3, only 6 bubbles became trapped by the time the foam flow reached the end of the 'observation' frame. It is only when the foam has had time to 'coarsen', where gas diffuses from smaller to larger bubbles (causing the smaller bubbles to disappear), that bubble trapping becomes more significant. The coarsening process can take up to 5 minutes in the current micromodel[1], so trapped gas measurements were therefore made after the flow was well established and steady state conditions were observed.

Variation in Trapped Gas with Position in Micromodel

The fraction of trapped gas in the micromodel, f_{gt}, was measured using the trapped bubble-fraction technique, was analysed as a function of position along the micromodel (Figure 4). The position was measured in the flow direction, along the longitudinal axis of the chip with x = 0 at the inlet. The measurements were carried out with a superficial velocity, u_t, of 0.14 m.s^{-1} and a foam quality, f_q, of 0.3. As can be seen there is very little variation in trapped gas fraction with position in the micromodel and there is no obvious entrance effect observed, as might be expected from the work in corefloods: Eftekhari et al.[12] observed elevated water saturations near the inlet of their core, and Ettinger and Radke[13] found that both the foam texture and the pressure profile varied near the core inlet, where foam generation

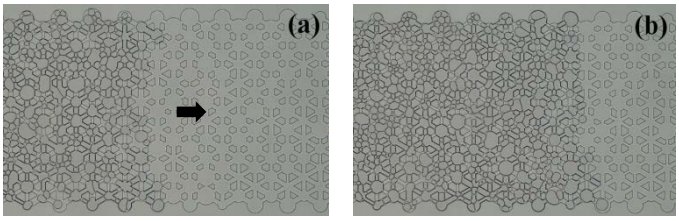

Figure 3 Plug flow of foam through an initially water saturated micromodel. The foam front is seen at a) t = 1 sec, b) t = 8.3 sec.

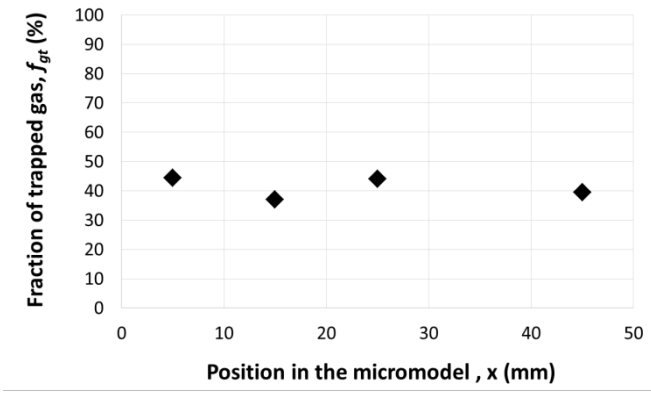

Figure 4 Trapped gas fraction as a function of position in the micromodel. Positions are defined with respect to the inlet of the micromodel. The measurements were carried out with a foam quality of 0.3 and a superficial velocity of 0.14 $m.s^{-1}$.

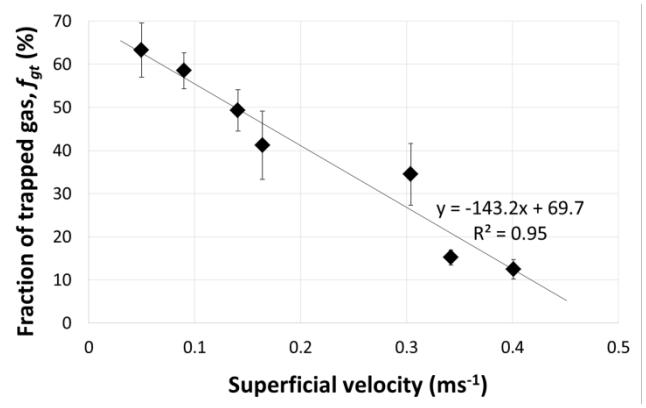

Figure 5 Trapped gas fraction as a function of the flow rate in the micromodel. Foam quality varies from 0.94 for the lowest flow rate to 0.98 for the highest flowrate. The error bars indicate the range of values obtained with small variations in the velocity thresholding.

mechanisms dominate. It is suggested that any entrance effect is very short in the current geometry, and at the high velocities considered, and is thus not observable in the current experiments.

Variation in Trapped Gas with Total Flow Velocity

Trapped gas fractions were measured, using the trapped bubble fraction technique, as a function of flow velocities (Figure 5) for foam qualities in the range of 0.94 to 0.98. It was found that trapped gas fraction decreases linearly with increasing flow velocity, with trapped gas fractions ranging from 65% down to 10%. Extending the trendline in Figure 5 back to the velocities typically found in core flood tests and EOR applications (~ 1 x 10^{-4} $m.s^{-1}$), we would predict a trapped gas fraction of approximately 70% at these velocities. This is in broad agreement with the previous tests in rock cores, where trapped gas fractions in the ranges 0.75-0.9[7], , 0.72 – 0.99[8] and 0.56 – 0.87[9] were measured. However, it is noted that the trapped gas fractions in the core floods are generally greater than the 70% predicted by the micromodel (Figure 5),

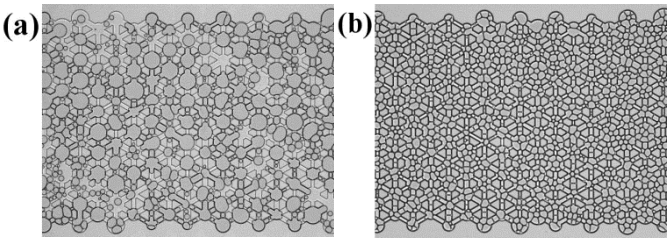

Figure 6 Images of the bubbles in the porous media for a) linear velocity of 0.09 $m.s^{-1}$ and b) 0.4 $m.s^{-1}$. There is a strong dependence of foam structure on the flow velocity. Average bubble size decreases with increasing velocity.

suggesting that the relationship between trapped gas and velocity becomes non-linear at the lowest velocities, with a predicted upswing in the trapped gas as $u_t \rightarrow 0$.

It was noted that this relationship between trapped gas fraction and velocity was strongly linked to the foam structure within the micromodel. At the lower flow rates, the residence time of the bubbles within the pores was higher, which allowed more time for coarsening. This resulted in a large proportion of the bubbles coarsening to the size of the pores (Figure 6a and Table 1). In general, once a bubble coarsens to the same size as a pore, the surrounding lamellae are found in very stable, low-energy configurations in the pore throats[14].

Table 1 Average bubble size and polydispersity for the two foams shown in Figure 6. The average pore diameter is 60µm, equivalent to an area of 2827 μm^2.

Linear Velocity ($m.s^{-1}$)	Number of Bubbles in Frame	Average Bubble Size (μm^2)	Standard Deviation (μm^2)	Polydispersity Index = St.Dev./Average
0.09	510	660	882	1.34
0.4	2566	265	181	0.68

The energy then required to move the lamellae out of the pore throats becomes significant and only an increase in the driving pressure[1,14] or lamella breakage will remobilise these pore-size bubbles. This results in a greater probability of bubbles becoming trapped long term at lower flow-rates, thus giving a higher trapped gas fraction.

At higher velocities, the average bubble size was much smaller than the average pore size (Figure 6b and Table 1) and the foam flow behaviour was more similar to a Newtonian fluid. There was less time for coarsening to occur as the residence time of bubbles at a fixed location was greatly reduced and there were continuous changes in nearest neighbours (thus disrupting the diffusion necessary for coarsening). The amount of trapped gas was therefore greatly reduced.

This result appears to be in direct contradiction to that of Tang and Kovscek[9], who found that higher gas velocities produced larger bubbles in the effluent. However, they also linked the larger bubble size to a reduction in trapped gas. So, both in the work of Tang and Kovscek[8] and in the current study it was found that higher velocities resulted in lower quantities of trapped gas.

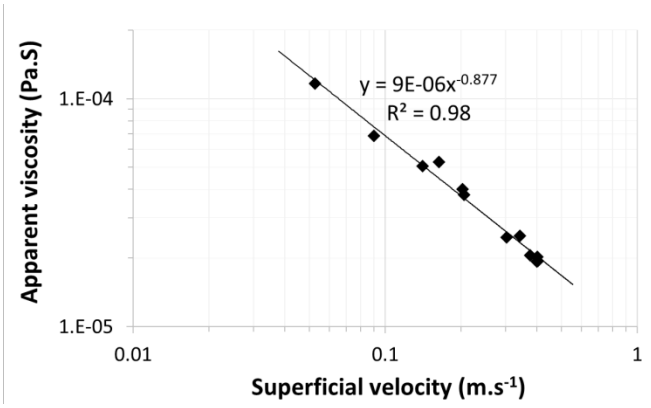

Figure 7a Measured apparent viscosity of the foam as a function of the total superficial velocity

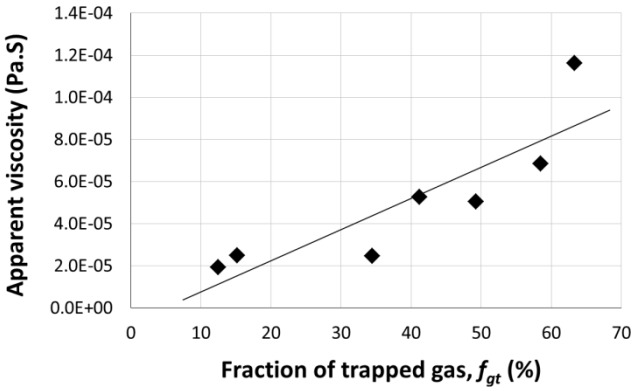

Figure 8 Variation in measured apparent viscosity with the trapped gas in the micromodel

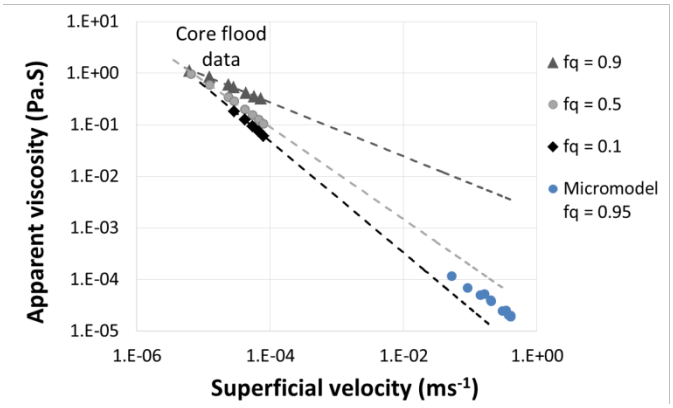

Figure 7b Extended version of the shear thinning curve, including data from shear thinning tests carried out locally in Bentheimer sandstone cores[15].

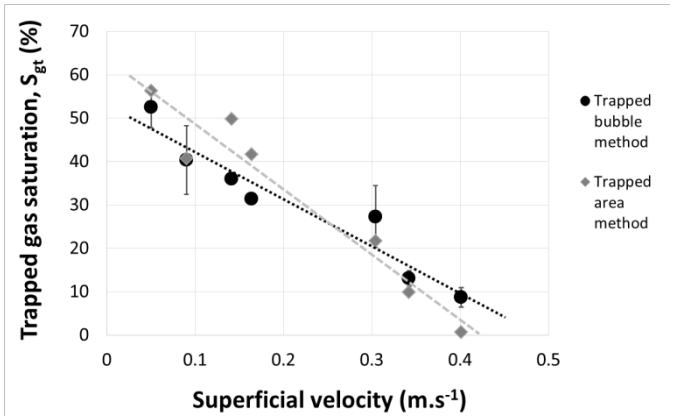

Figure 9 Trapped gas saturation, measured using the trapped area and the trapped bubble techniques, plotted as a function of the superficial velocity. The error bars in the trapped bubble fraction measurements indicate the range of values obtained with small variations in the velocity thresholding.

Shear Thinning Behaviour

The shear thinning behaviour of the foam in the micromodel was determined by measuring the apparent viscosity of the foam as a function of the total superficial velocity. The apparent viscosity of the foam, $\mu_{foam,app}$, could then be calculated using Darcy's law:

$$\mu_{foam,app} = \frac{k\nabla P}{(u_l + u_g)} \quad (6)$$

where ∇P is the pressure gradient across the micromodel [Pa.m^{-1}] once steady state was achieved, u_l and u_g are the liquid and gas superficial velocities respectively [m-s^{-1}], and k is the permeability of the micromodel (0.72 Darcy).

The apparent viscosity was found to vary with the injection flow rate as shown in Figure 7a, following a typical shear-thinning power-law curve with an exponent of -0.877 (shear thinning curves in Bentheimer rock cores have been found to have exponents in the range -0.5 to -1.0, depending on foam quality[15]). It is noted that the calculated viscosities have very low values, compared to typical foam measurements, but this is linked to the high velocities (~0.5 m.s^{-1}) used in this test which are significantly higher than those found in typical core flood experiments (~10^{-5} m.s^{-1}). However, there is still a definite link between the behavior in the micromodel and the behavior in a core flood, as shown in Figure 7b, where the data over the whole range of velocities are plotted together. The trend lines for the core flood data are extended up to the micromodel velocities and give a good prediction of the low viscosities measured in the micromodel. It is acknowledged that there are some discrepancies in this prediction, especially with regards to matching the foam quality in the core flood and the micromodel, but, as discussed in full later, there are several structural differences (size, roughness etc) between the micromodel and sandstone.

It is suggested that one of the reasons for the strong shear thinning response of the foam flow in a porous media is the variation in the quantity of trapped gas with velocity (Figure 5). The higher the quantity of trapped gas, the fewer the number of available flow paths within the medium. This results in a higher resultant pressure gradient, which gives a higher value of measured apparent viscosity. Considering how the apparent viscosity varies with the quantity of trapped gas in the micromodel (Figure 8), it can be seen that there is a strong correlation between the two quantities.

Comparison of Trapped Gas Measurement Techniques

The quantity of trapped gas in the micromodel was determined using the two measurement techniques: firstly, the trapped area fraction (giving S_{gt}) calculated via image analysis, and secondly the trapped bubble fraction (giving f_{gt}) calculated via consideration of the bubbles' velocities, over a range of different velocities. In order to make a good comparison, the values of f_{gt} for the trapped bubble technique were converted to saturations using equation 1 and estimates of S_w (determined from the images of the foam). A comparison of the resultant trapped gas saturations for the two techniques are shown in Figure 9.

It was found that there was good agreement between the two measurement techniques, although there is a slight difference in the gradients of the resultant trend lines. It should be noted, however, that there are errors inherent with both of the techniques, which would account for the scatter in the data. Considering the trapped area measurement, the calculations from the composite image (Figure 2) assume that all flowing paths are completely filled by the superimposed images of lamellae, when in fact there are gaps. This would then result in an overestimation of the trapped gas saturation. Considering the trapped bubble fraction measurement, there are difficulties in setting an appropriate velocity threshold. If the velocity threshold is set too high, the trapped gas fraction will be overestimated by slow moving bubbles also being counted as trapped. And if the velocity threshold is too low, bubbles that are trapped, but oscillating in place (with a resultant significant velocity), will not be counted as trapped. The error bars in Figure 9 give an indication of the range of different values that can be obtained with small variation in the velocity thresholding. In both cases, errors could also be introduced into the measurements of the trapped gas due to the effect of fluctuating flow paths[6].

Results and Discussion – Trapped Gas Model

Effect of the Trapped Gas on Relative Permeability

The gas relative permeability k_{rg} was calculated in two different ways: 1) based on the trapped gas saturation S_{gt} measurements, from eqn. 3; and 2) from the apparent viscosity of the foam μ_{foam}, from eqn. 5. The data used for the comparison was from the microfluidic experiments, with superficial velocities varying from 0.05 to 0.4 $m.s^{-1}$ (see Figure 9). As can be seen in Figure 10, the results showed a linear trend of $k_{gr}(S_{gt})$ with relation to $k_{rg}(\mu_{foam})$, which would indicate that trapped gas S_{gt} is correlated with μ_{foam}.

However, the data is very scattered (R^2 = 0.69 for the trendline), and there are several factors that could have caused this. Firstly, the measurements of S_{gt} were carried out on only a small section of the micromodel, limited by the field of view of the microscope (~ 1mm), as compared to the apparent viscosity measurement which is based on the pressure drop over the full length of the micromodel (6 cm). Thus localized S_{gt} measurements are compared with bulk μ_{foam} measurements, and there is an associated greater degree of scatter in the localized measurements. Secondly, the Corey

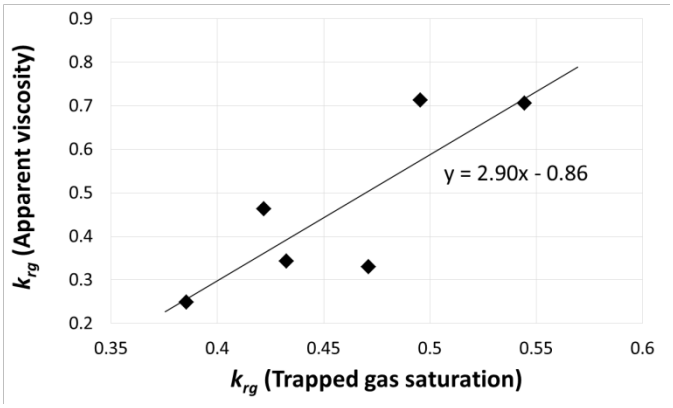

Figure 10 Gas relative permeability k_{rg} calculated from the foam apparent viscosity μ_{foam}, (equation 5) plotted as function of k_{rg} calculated from the trapped gas S_{gt}, (equation 3).

parameters and end-point relative permeability used in the calculations (eqn. 3) were taken from measurements of Bentheimer sandstone with a similar permeability to the micromodel[11]. However, there are several structural differences between the micromodel and the sandstone. The micromodel is a 2-D system, with smooth glass walls, a very high porosity (~ 0.58) and an average pore diameter of 60µm (with standard deviation of 11 µm, giving a PDI of 0.18). In contrast the Bentheimer is a 3D system of irregular grain, lower porosity (~ 0.23) and much wider pore size distribution[1] (average pore diameter of 22 µm with standard deviation of 28 µm, giving a PDI of 1.25). Any of these structural differences could potentially alter the Corey parameters and end-point relative permeabilities, and it is suggested that future work should involve measurement of the actual Corey parameters for the micromodel, to improve the accuracy of the model.

Also, it is noted that the slope of the trend in Figure 10 should be 1 if both equations 3 and 5 accurately describe k_{rg}. However, the slope in the current work is approximately 3 (with R^2 = 0.69). It is suggested that this discrepancy is again partly due to the localized/bulk measurement and Corey parameters discussed above. There is also the possibility that there is a constant is missing or inaccurate in equations 3 or/and 5.

Conclusions

Foam flow tests have been carried out in a 2D micromodel to investigate the trapped gas behavior within a porous media. Significantly, the trapped gas fraction of the foam was measured directly. Two different techniques were used to determine the fraction of trapped gas in the micromodel: firstly, a trapped bubble technique, based on velocity thresholding of the foam flow, and secondly, a trapped area technique, based on image analysis. The two techniques were in good agreement, and the following observations have been made:

There are errors inherent with the two trapped gas measurement techniques, both in the image analysis and the

velocity thresholding. However, these errors are in general small, and both of the trapped gas measurement techniques are capable of showing the foam response to changing conditions. It is suggested that either technique would be suitable for future tests, although individual experimental set-ups may bias towards a particular technique.

It is important to note that the two techniques measure slightly different quantities. The trapped area technique makes a direct measurement of the trapped gas saturation, S_{gt}, and the trapped bubble technique measures the trapped gas fraction, f_{gt} (which can be used to calculate the saturation if the total gas saturation, S_g, is known).

If the foam quality and flow velocity were kept constant, there was no significant difference in trapped gas fraction regardless of the position in the micromodel. There was no observable entrance effect at the flow velocities tested.

Considering the flow velocity, there was a strong response of the trapped gas to variations in the foam velocity. The trapped gas fraction dropped from 63% to 12% as the velocity increased from 0.05 to 0.4 $m.s^{-1}$. Increasing the total velocity resulted in a reduction of the trapped gas fraction, and this could be linked to the changing foam structure observed at the different flow velocities. Higher flow rates produced finer textured foams that were less likely to block individual pores. At lower flow rates, there was a higher probability of bubbles coarsening to the size of the containing pore; a very stable configuration that would greatly increase the chance of the bubble becoming trapped long term.

It is suggested that a similar effect will be observed if the foam quality is varied with constant total flow velocity. The gas fractional flow rate will be low at the lower foam qualities, implying that coarsening, and hence gas trapping, will be more likely. And high gas flow rates at high foam qualities would imply lower trapped gas fractions. Ongoing tests are currently being carried out to investigate this effect.

The foam flow also showed strong shear thinning behavior, consistent with behavior previously observed in core-flood studies[16]. There is a strong correlation between the shear thinning behavior and the trapped gas within the system.

The trapped gas model was used to calculate the effect of the trapped gas on the gas relative permeability, using both the trapped gas saturation S_{gt} measurements (eqn. 3) and the apparent viscosity of the foam μ_{foam} (eqn. 5), and the following observation were made:

A linear trend was observed of $k_{gr}(S_{gt})$ against $k_{rg}(\mu_{foam})$, which would indicate that trapped gas S_{gt} is correlated with μ_{foam}. This would suggest that the apparent viscosity of the foam is mainly due to the trapped gas.

There was a large degree of scatter in the model data. This could be partly attributed to the fact that the trapped gas saturations, S_{gt} , measurements were highly localized and the apparent viscosity measurements were based on the pressure drop over the whole micromodel i.e. averaged over any localized variations in the trapped gas saturation.

The Corey parameters and end-point relative permeability used in the model were taken from data for Bentheimer sandstone with a similar permeability to the micromodel. However, there are structural differences between the micromodel and the sandstone, and it is suggested that future work should involve measurement of the actual Corey parameters for the micromodel, to improve the accuracy of the model.

Acknowledgements

We would like to acknowledge the financial support from Shell Global Solutions International B. V., and the technical support from Michiel Slob. We thank Dr. Evren Unsal for her careful review of the manuscript and useful comments.

Notes and references

1 S.A. Jones, N. Getrouw and S. Vincent-Bonnieu, Soft Matter, 2018, DOI: 10.1039/C7SM01903C
2 A.H. Falls, J.J. Musters and J. Ratulowski, *SPE Reservoir Engineering*, 1989, **4**, 155-164.
3 A.R. Kovscek, T.W. Patzek and C.J. Radke, *SPE/DOE Improved Oil Recovery Symposium*, Tulsa, Oklahoma, 1994, SPE-27789-MS.
4 A.R. Kovscek and H.J. Bertin, *Transport in Porous Media*, 2003, **52**, 17-35.
5 Q.P. Nguyen, W.R. Rossen, P.L.J. Zitha and P.K. Currie, *SPE Journal*, 2009, **14**, 222-236.
6 R.A. Kil, Q.P. Nguyen and W.R. Rossen, *SPE Journal*, 2011, **16**, 24-34.
7 F. Friedmann, W.H. Chen and P.A. Gauglitz, *SPE Reservoir Engineering*, 1991, **6**, 37-45.
8 C.J. Radke and J.V. Gillis, *SPE Annual Technical Conference and Exhibition*, New Orleans, Louisiana, 1990, SPE-20519-MS.
9 G.-Q. Tang and A.R. Kovscek, *Transport in Porous Media*, 2006, **65**, 287–307.
10 W.S. Rasband, ImageJ, U. S. National Institutes of Health, Bethesda, Maryland, USA, http://imagej.nih.gov/ij/, 1997-2016.
11 L .Kapetas, S. Vincent-Bonnieu, R. Farajzadeh, A.A. Eftekhari, S.R. Mohd-Shafian, R.Z. Kamarul Bahrim and W.R. Rossen, *Colloids and Surfaces A: Physicochemical and Engineering Aspects*, 2017, **530**, 172-180.
12 A.A. Eftekhari, R. Krastev, and R. Farajzadeh, *Ind. Eng. Chem. Res.*, 2015, **54**, 12482–12491.
13 R.A. Ettinger and C.J. Radke, *SPE Reservoir Engineering*, 1992, **7**, 83–90.
14 L.E. Nonnekes, S.J. Cox and W.R. Rossen, *Transport in Porous Media*, 2014, **106**, 669-689.
15 S.A. Jones and S. Vincent-Bonnieu, Unpublished work
16 R.K. Prud'homme, *Foams: Theory, Measurements, Applications* (Vol. 57), CRC Press, 1995.